

# INTERNATIONAL SPACE STATION AGRICULTURAL CAMERA (ISSAC) SENSOR ONBOARD THE INTERNATIONAL SPACE STATION (ISS) AND ITS POTENTIAL USE ON THE EARTH OBSERVATION

Ho Jin Kim\*, Douglas R. Olsen, and Soizik Laguette

Dept. of Earth System Science and Policy, John D. Odegard School of Aerospace Sciences  
University of North Dakota, 4149 University Ave., Grand Forks ND 58202-9011  
Tel. 701-777-4450, Fax 701-777-2940  
email: [hkim@ad.ndus.edu](mailto:hkim@ad.ndus.edu)

## ABSTRACT

Recently launched and installed inside the Window Observational Research Facility (WORF) in the International Space Station (ISS), the International Space Station Agricultural Camera (ISSAC) sensor is an area-scan multi-spectral optical imaging system built by students and faculty at the University of North Dakota (UND). Radiometric calibration was conducted before launch and performance validation was evaluated with radiance extracted from Landsat5 TM image that was overpassed nearly at the same time as ISSAC overpass. Ground truth measurement with Analytical Spectral Devices (ASD, ASD Inc., Boulder CO) was also carried out over fairly homogenous regions of interest such as bare soil, gravel parking lot, crop and short grass pastures. Using the 6S radiative transfer model, radiances measured at the top-of-the atmosphere were converted into surface reflectance. Atmospheric corrected surface reflectance from ISSAC images was compared with the spectrum of ground ASD measurement. The results for both radiance and surface reflectance show fairly good agreements. This indicates that ISSAC would be a prospective candidate that would be able to fill the temporal gaps of Landsat 16-day revisit cycle. Higher rate of temporal opportunities from ISSAC sensor will result in significant improvement on decision making for users especially in time sensitive disaster management, farming practices or environmental issues occurred in short time frame.

**Keywords:** International Space Station, radiance, reflectance, radiometric validation.

## INTRODUCTION

ISSAC sensor is a multispectral instrument designed to acquire three spectral bands in green, red, and Near-Infrared (NIR) with higher temporal frequency. The imaging system has been developed by students and faculty in the University of North Dakota at low cost budget. The system is installed inside the Window Observational Research Facility (WORF) in the International Space Station (ISS), optical window on the ISS. In order to keep costs low, ISSAC used commercial-off-the-shelf (COTS) products. Electro-optical components of ISSAC include an f/4 Sigma 150 mm lens (APO EX-DG Macro HSM), a beam splitter, and three two digital area scan cameras (Basler AG, Germany). ISSAC is capable of pointing in a cross-track direction of up to  $\pm 30^\circ$ , enabling multiple revisits of a target during a short time period. The ISS orbits at 51.6 degree inclination, with an altitude that varies between 350 and 420 km. Orbital speed varies accordingly; a nominal velocity of 7,220 m/s at 400 km altitude. The imaging system features three  $1392 \times 1040$  CCD arrays of spectral bands of green, red, and near infrared (NIR) with 12-bit quantization. Ground foot print is about 21.5 km x 16 km with ground sample distance of 20 m at a nominal ISS altitude of 350km above sea level. With capability of  $\pm 30$  degrees off-nadir pointing angle ISSAC provides frequent images on applications of disaster response and agricultural practices with possibilities of multiple times a day to a week to users. Due to its spectral similarity, we examined radiometric performance of the ISSAC sensor and compared results of several targets extracted from Landsat Thematic Mapper(TM). Pre-launch sensor characterization was conducted at NASA AMES research center, Moffett field, CA including determination of spectral bandpasses of three spectral bands; green, red, and NIR, measurement of radiometric responsivity with 30-inch NIST calibrated integrating sphere, and characterization of flat field through entire field of view. Following laboratory characterization, field measurements of few ground targets were conducted to validate radiometric performance of the ISSAC sensor. This paper reports on experimental and validation work of the radiometric calibration and the first results from ground truth validation of in-flight condition of the sensor.

## SPECTRAL & RADIOMETRIC CALIBRATION

### Sensor Pre-launch Radiometric Calibration

In order for data to be comparable, remote sensing sensor must be calibrated. In addition, calibration of the sensor must be validated in on-orbit environment after launch to investigate any performance change due to launch vibration, in microgravity and in different radiation environment. For pre-flight characterization of the ISSAC sensor, spectral and radiometric calibration was conducted in collaboration with the Airborne Sensor Calibration Laboratory (ASCL) at the NASA Ames Research Center located in Moffett field, CA. Sensor pre-launch calibration performed includes (1) spectral bandpass determination (2) radiometric responsivity of output digital counts corresponding to known input radiance, and (3) CCD array variance and lens fall-off characterization (Olsen *et al.*, 2011).

Spectral characterization was performed using an Oriel 7345 tunable narrowband monochromator (figure 1). The FWHM for the collimated light is 5 nm. A full spectrum scan was first performed to validate the bandpass of the trim filters. Next, spectral response for each camera was determined every 5 nm. Before and after each measurement, reference spectra were recorded using a calibrated silicon photodiode to monitor the stability of the light source. The spectral responses of ISSAC sensor show in Figure 1.

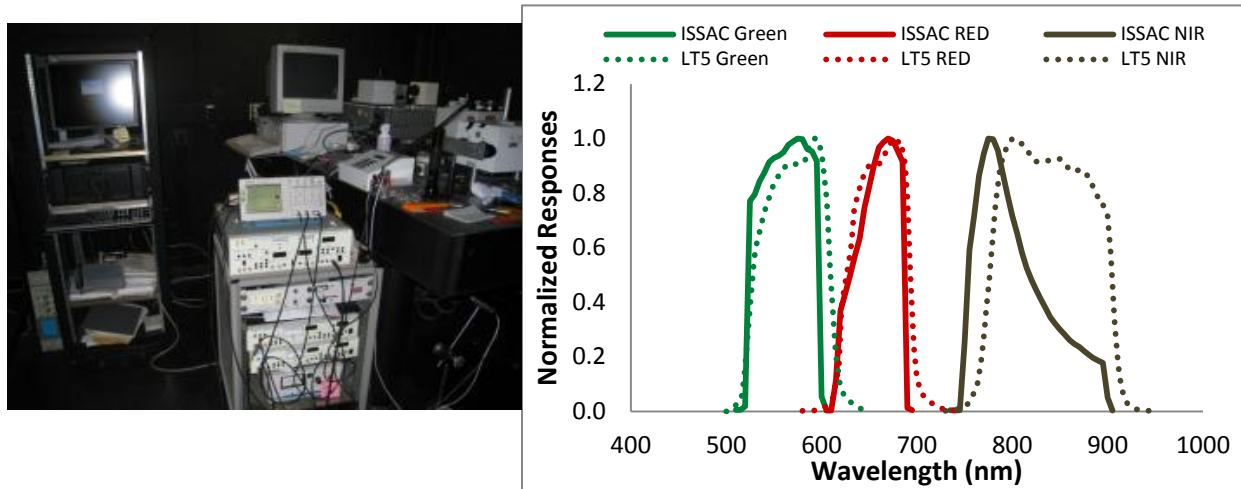


**Figure 1.** Tunable monochromator used to measure spectral band passes (left). Normalized spectral responses of the three ISSAC bands and its comparison with Landsat5 TM spectral bands.

Radiometric characterization was performed using a 30 inch diameter 12-bulb integrating sphere. The sphere contains twelve 45 W lamps operated at a nominal 6V (Steven *et al.*, 2005). The integrating sphere is coated on its inside surface with barium sulfate and provides spectral range of 350-2500nm. The lamps are controlled by twelve short switches assigned to each corresponding lamp. Individual lamp voltage and currents are displayed on the control switch panel. The sphere has a 10 inch diameter aperture emitting upward direction. The instrument is calibrated on a periodic basis to a traceable radiometric source to the U.S. National Institute of Standards and Technology (NIST) standard of spectral irradiance. The light bulbs were turned on successively and the camera took images looking into the integrating sphere cavity at each level until saturation. The absolute radiance at each bulb level was measured at 10 nm spectral interval for calibration purpose on Sep. 15, 2010. The spectra were used to calculate absolute response by convolving ISSAC spectral bands.

Figure 2 shows NASA AMES 30 inch integrating sphere and absolute radiance of AMES integrating sphere and output spectral response variation measured by ISSAC sensor. The absolute radiance of the integrating sphere was calibrated on the very next day, September 10, 2010 using a NASA NIST traceable source. Detector responses at different lamp level were convolved using three ISSAC spectral band passes. DN output was also measured at corresponding radiance input from the integrating sphere.

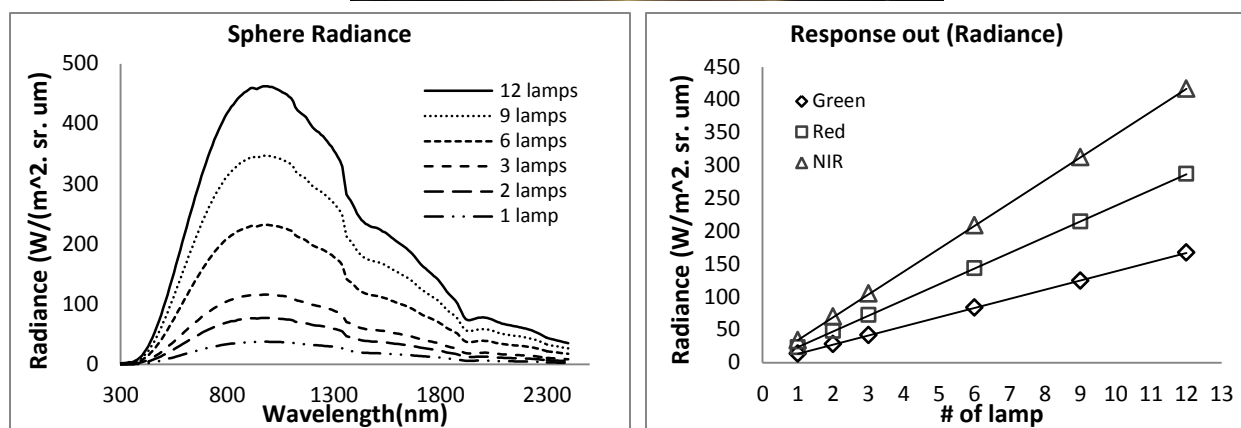
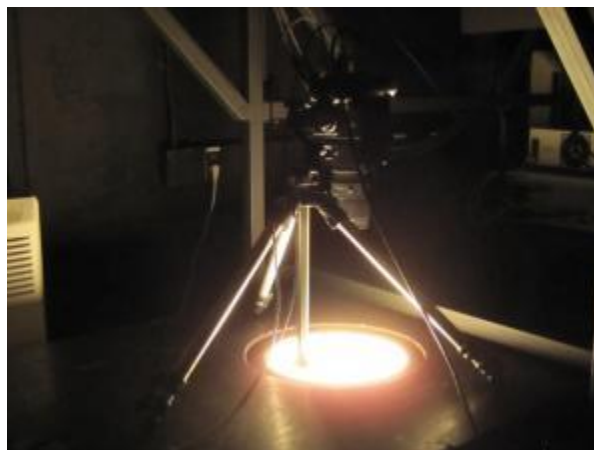


**Figure 2.** NASA AMES 30 inch integrating sphere with ISSAC sensor looking down to the sphere aperture (top). AMES Integrating sphere absolute radiance of 1, 2, 3, 6, 9, and 12 lamp level (bottom left) and output radiance convolved to three ISSAC spectral band (bottom right).

With following equation, raw Digital Number (DN) is converted radiance at the sensor in unit of Watt/(m<sup>2</sup>·sr·μm) and vice versa.

$$\text{Radiance (at sensor)} = [\text{DN} \times \text{Calibration gain} + \text{Offset}] * \text{TW} \quad (1)$$

TW represents transmittance of the US Laboratory window, as measured during pre-flight characterization. Pre-flight optical transmittance of the window was measured by NASA; transmittance in the green, red and NIR band of ISSAC is estimated to be 95.53%, 97.48%, and 93.30% respectively (Scott *et al.*, 2003).

In order to investigate scene artifacts and lens falloff effect, uniform target imagery was obtained from a flat-field uniform source, which uses diffuse glass emission plate with multiple reflective internal baffles between the output plate and an adjustable stable bulb source. The exiting light field is within 1% Lambertian for angles up to 30 degrees. Placement of the ISSAC sensor within a few centimeters of the output diffuser further improved quality of the exiting light field, as near-field de-focus effects averaged any residual source variations from dust or other minor source defects.

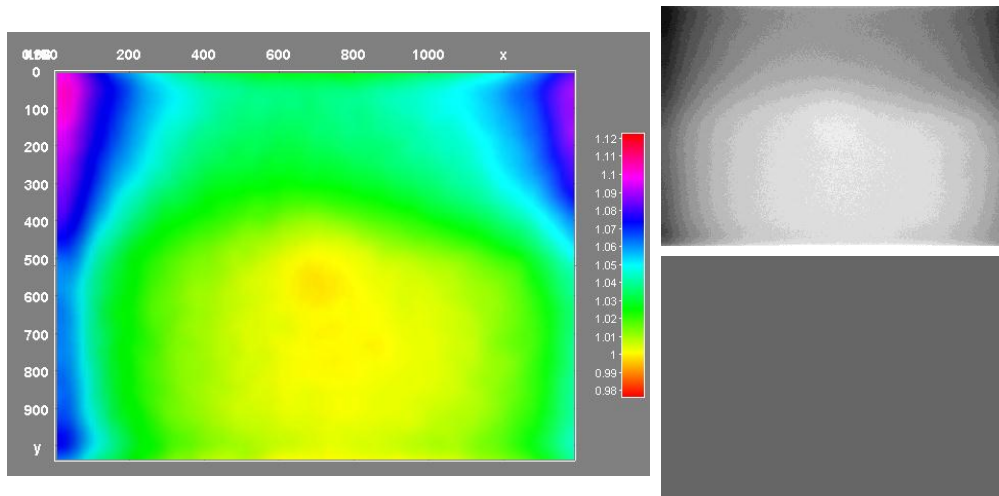


**Figure 3.** Flat field coefficients distribution through a detector array and its application to an image, picture shows green band example. A grey scale image taken in front of flat field device in green band (upper right) and after correction applied (bottom right)

### Radiometric Calibration Validation

First, radiance conversion was applied to images of ISSAC and Landsat5 TM scenes acquired near El Paso, TX . The images were acquired only a few seconds apart, with ISSAC at nadir viewing angle, resulting in negligible differences in sun-sensor-target geometry and atmospheric conditions.. Four different targets were extracted from vegetated cover and bare soil. Radiometric calibration was applied to a Landsat5 TM image obtained from USGS EROS center[1]. Radiometric conversion procedure was same except multiplying the window transmittance coefficients. Figure 4 shows a scatterplot of radiance comparison between ISSAC and Landsat. A number of pixels were extracted from the targets and simple average was applied. Due to the difference of spatial resolution between two sensors, averaged pixel numbers are slightly different. Radiance of red and green bands shows quite good agreement. NIR band shows slight deviation from 1:1 line. At lower brightness targets, higher radiance was observed with ISSAC sensor, but observed higher radiance from Landsat image at brighter targets. Possible source of the deviation observed in NIR band might be due to spectral bandpass differences (Tiellet *et al.*, 2007). Spectral response in NIR band of ISSAC sensor seems to be shifted toward shorter wavelength compare to NIR band of Landsat5 TM and somewhat narrower than that of Landsat5 TM.

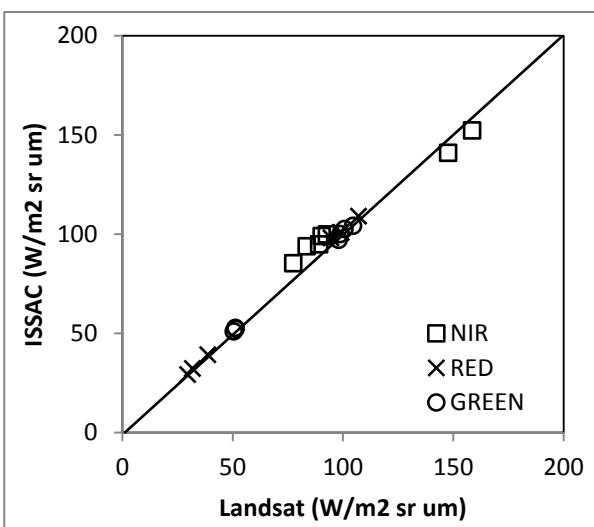


**Figure 4.** Radiance comparison between ISSAC and Landsat5 TM. Radiance extracted from both images acquired at a location about 20 miles SE of El Paso, TX along the US-Mexico border.

### Atmospheric Correction

Signals from satellite imagery data are degraded by a result of atmospheric attenuation with scattering and absorption. These atmospheric effects depend on the wavelength of the imaging sensor system and vary spatially and temporally. The Second Simulation of the Satellite Signal in the Solar Spectrum (6S) is a radiative transfer code developed by Vermote *et al.*, (1997) and simulates the effect on the radiation transferred through the Earth's atmosphere in the spectral range 0.25-4.00  $\mu\text{m}$ . The 6S code simulates the effect of the atmosphere in the signal due to atmospheric attenuation by scattering by molecules and aerosols and by absorption - mainly by H<sub>2</sub>O, CO<sub>2</sub>, O<sub>2</sub>, O<sub>3</sub>, CH<sub>4</sub>, and N<sub>2</sub>O (Vermote *et al.*, 2006). The input parameters include the viewing and

illumination geometry, atmospheric model for the gaseous components, aerosol model, visibility, sensor/band information, and surface condition. The 6S code computes the TOA radiance or reflectance corresponding measured value on the ground. The input information on atmospheric conditions is the same as in the situation described above, but no BRDF are considered apart from a Lambertian target assumption. The surface condition in this work is assumed homogeneous and no bi-directional reflectance effect was considered. Two simple cases were compared; one using default gas/aerosol model and another using column water vapor and ozone contents obtained from MODIS atmospheric products, level 2. MODIS is a scanning sensor having 36 spectral bands. The MODIS level 2 products, MOD07 provide precipitable water vapor amount and several atmospheric indices including aerosol and ozone contents at 1km spatial resolution on the ground

For ground validation, spectral data of five ground targets were collected using ASD FieldSpec3 portable spectroradiometer (ASD Inc, Boulder, CO) nearly at the same time as ISSAC overpass at 18:27:38 on September 7, 2011. Spectra collection was started 30 minutes ahead and last about an hour. Time difference between image acquisition and ground spectra measurement was within  $\pm 30$  min and atmospheric effects would be negligible. The spectroradiometer is characterized by 1.4nm sampling interval from 350nm to 2500nm with a spectral resolution of 3 nm. The sampling interval from 1050 - 2500nm is 2nm with the spectral resolution between 10nm and 12 nm. The resulting spectrum are then resampled to 1nm interval using the ASD software. Spectrum samples were collected with a continuous mode acquiring every 1 sec interval with 25 degree field of view at a height of 1 m above ground which cover ground circular area with a diameter of about 0.45m. Prior to target sample collection, the radiance of a standard panel coated with barium sulfate, spectralon (Labsphere, Boulder, Inc) was recorded for target spectrum normalization. Parallel line transects were drawn visually across entire width of the targets. Three ground targets samples, gravel parking lot, green turf grass, and drying grass were collected in Wahpeton, ND on September 5, 2011 and two samples at a sugarbeet farm field and harvested wheat stubble field with with sparse crop residue in Manvel, ND on September 7, 2011. About 1000 spectrum were collected for each target and the spectrum are averaged. Two ISSAC images acquired almost at the same time of ground sample collection and atmospheric correction was performed using 6S in two atmospheric conditions. Figure 5 shows the results of surface reflectance spectral signature and comparison between ground measurement and ISSAC atmospheric correction.

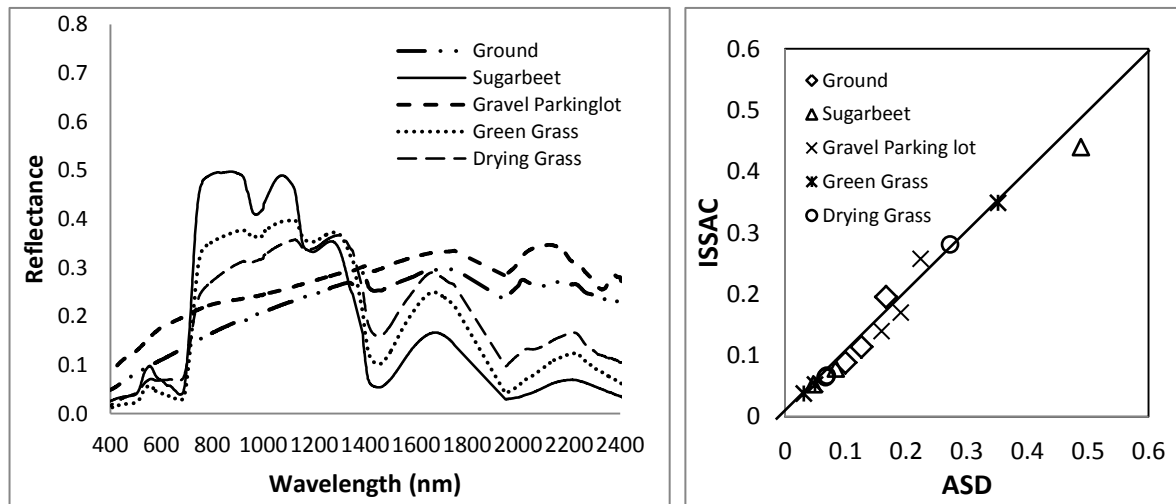


**Figure 5.** Spectral signatures of the ground targets measured by ASD spectroradiometer (left). Comparison of the surface reflectance between measured by ASD and corrected signal from an ISSAC image (right).

### Image Processing and Data Products

Custom software written in Interactive Data Language (IDL) was developed to perform in-house image processing. The ISSAC project will deliver three types of Level-1 data products: Level-1R, Level-1G0 and Level 1A, as is illustrated in Figure 6. Raw imagery data consists of acquired data that has been downlinked via a packetized telemetry stream and rebuilt (de-packetized) into individual single-band (green, red, near-infrared) 12-bit images, in a track-down orientation (direction of flight is at the bottom of the image). The Level-0 product is rotated to track-up orientation, and band-band co-registered into a single 3-band stacked .tif format image. The Level-1R

product has radiometric calibration coefficients applied to produce scaled radiance at the sensor. Level-1G0 data has coarsely-determined latitude and longitude information embedded by using parameters of the spacecraft attitude, ephemeris, and sensor viewing angle to first establish geo-location to within a few kilometers. Level-1A is a product with atmospheric correction applied to Level 1G0 data to produce surface reflectance image. Entire processing steps are performed with minimal operator's intervention such as selecting input files or parameters at initial processing stage.

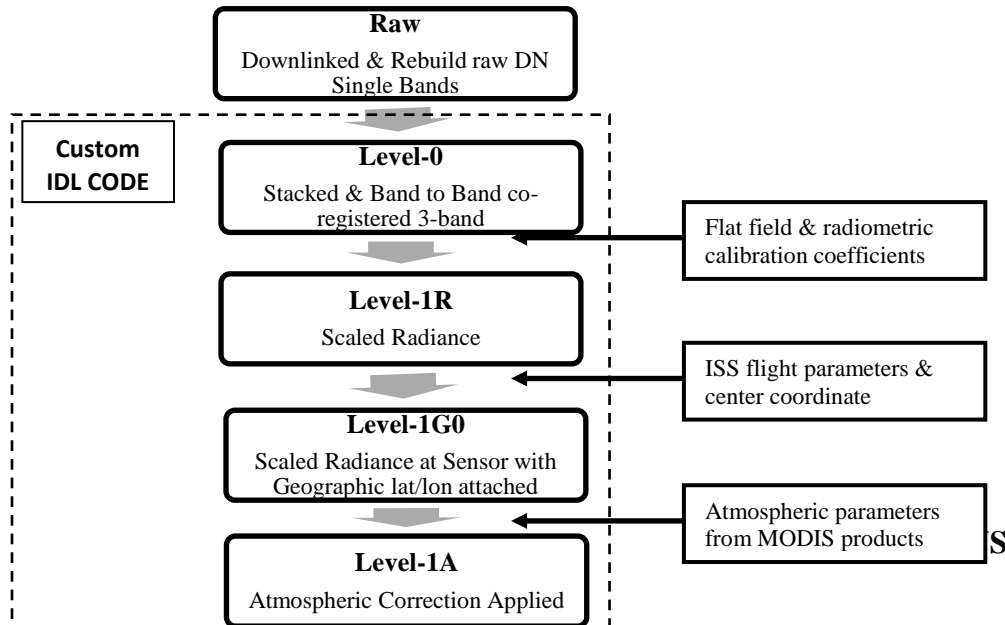


**Figure 6.** Schematic diagram of processing steps of ISSAC image. The code was written in IDL language

This paper provides calibration and validation of the ISSAC sensor to investigate onboard imaging performance. Pre-launch sensor calibration was validated with a Landsat image and ground spectroradiometer measurement. Spectral radiance and reflectance from ISSAC image show promising results for future use in filling gaps of Landsat repeat cycle. With its wide range of viewing capacity, ISSAC also seems to be quite helpful in the area that needs fast turn-around time such as agricultural application, disaster response, or environmental issues.

## ACKNOWLEDGEMENT

The authors acknowledge the support of NASA AMES Research Center Airborne Sensor Calibration Laboratory for providing invaluable resources for the ISSAC sensor calibration. This study was supported by NASA, grant #NNX08AO97G.

## REFERENCES

- Chander, G. and Markham, B.L., 2003. Revised Landsat-5 Thematic Mapper Radiometric Calibration Procedures and Postcalibration Dynamic Ranges. *IEEE Transactions on Geoscience and Remote Sensing*, 41(11): 2674-2677.
- Olsen, D. Kim, H.J., Ranganathan, J. and Laguette, S., 2011. Development of a low-cost student-built multi-spectral sensor for the International Space Station, *Proceedings of SPIE 8153*, 81530O.
- Steven W. Brown, B. Carol Johnson, Stuart F. Biggar, Edward F. Zalewski, John Cooper, Pavel Hajek, Edward Hildum, Patrick Grant, Robert A. Barnes, and James J. Butler., 2005. Radiometric validation of NASA's Ames Research Center's Sensor Calibration Laboratory, *Applied Optics*, 44(30):6426-6443.

- Scott, K., Biggar, S., Eppler, D., Zalewski, E., Brownlow, L., and Lulla, K., 2003. International Space Station Density Module Science Window Optical Characterization, *30th International Symposium on Remote Sensing of Environment*, Honolulu, HI.
- Teillet, P.M., Fedosejevs, G., Thomec, K.J. and Barker, J.L., 2007. Impacts of spectral band difference effects on radiometric cross-calibration between satellite sensors in the solar-reflective spectral domain. *Remote Sensing of Environment*, 110(3):393-409.
- Vermote E.F., Tanré D., Deuzé J.L., Herman M., and Morcrette J.J., 1997. Second Simulation of the Satellite Signal in the Solar Spectrum: an overview, *IEEE Transactions on Geoscience and Remote Sensing*, 35(3):675-686.
- Vermote E., Tanré, D., Deuzé, J.L., Herman, M., Morcrette, J.J. and Kotchenova, S.Y., 2006. Second Simulation of a Satellite Signal in the Solar Spectrum User Guide Version 3.